AIAA 2002-0199

Electrode Boundary Conditions in Magnetogasdynamic Flow Control

J. Poggie and D. V. Gaitonde
US Air Force Research Laboratory
Wright-Patterson AFB, OH 45433-7521

40th Aerospace Sciences Meeting & Exhibit
14-17 January 2002 / Reno, NV

Electrode Boundary Conditions in Magnetogasdynamic Flow Control

J. Poggie* and D. V. Gaitonde†
US Air Force Research Laboratory
Wright-Patterson AFB, OH 45433-7521

Preliminary results are presented from a study of plasma sheaths at the surface of electrodes immersed in hypersonic flow. A two-dimensional numerical code was written in which the conservation laws of fluid dynamics were solved with an explicit finite difference scheme and a Poisson equation for the electric potential was solved simultaneously using an SOR/ADI method. Three example problems were considered: a transient plasma sheath in the collisionless, cold-ion regime, an analogous sheath in the diffusion regime, and a supersonic, laminar, boundary layer flow over a cathode. Good agreement was found between the collisionless sheath computation and a solution available in the literature. A significant voltage drop and temperature rise were observed in the electrode boundary layer flow; these effects are expected to be important in flow control applications. Future work will focus on implementing an implicit numerical scheme, and on enhancing the fidelity of the physical model.

Introduction

INTEREST in electromagnetic control of hypersonic flows dates to the mid-1950s, when the problem of an aerospace vehicle entering the atmosphere from space was first being explored. Given the high temperatures in the shock layer around such a vehicle, and the concomitant ionization and electrical conductivity, it was natural to consider exploiting electromagnetic effects for flow control.[1] A number of successes were achieved in this era, including experimental confirmation of a shock stand-off increase,[2] heat transfer reduction,[3] and drag increase[4] with the application of a magnetic field to hypersonic blunt body flows. Interest nevertheless waned due to the success of conventional thermal protection systems and the weight penalty of magnetic systems.[5] Large, heavy magnets would have been required to provide magnetic fields sufficiently strong to affect the flow at the relatively low electrical conductivity corresponding to 'natural' thermal ionization in reentry flows.

The field has recently been revived with experimental work on shock propagation in weakly-ionized, non-equilibrium plasmas,[6,7] and the disclosure of the Russian AJAX vehicle concept.[8] Early on, some researchers proposed that the presence of the plasma could, in itself, be used to modify a shock, but the current consensus is that thermal effects dominate for the low levels of ionization present in this class of experiments. So far, whenever comparisons have been carried out between experiments and gasdynamic computations, no significant discrepancies have been found.[9–12]

It now seems that electromagnetic control techniques will have to utilize 'artificial' ionization and light-weight magnets. The most promising possibilities for electromagnetic control probably lie in applying control where the 'leverage' is greatest: mitigating at a local level the seemingly intractable thermal loads associated with hypersonic flight. Of particular interest are the regions of unsteady flow separation in the vicinity of control surfaces and excessive combustor temperatures in SCRAMJET engines.

Over the past few years we have been developing a set of computational tools to study possible electromagnetic flow control techniques. (See Refs. 13–15 for related work by other research groups.) In past work we have developed a magnetogasdynamic code suitable for computations at both relatively high[16] and low[17] magnetic Reynolds numbers, and have examined the use of magnetic forces to extract energy from the flow and to reduce temperature and heat flux.

If the imposed magnetic field is combined with electrodes at the body surface, it should be possible to obtain a stronger effect and to add or extract flow energy. To examine this type of control, we have now included in the code the capability to compute, in the quasi-neutral, low magnetic Reynolds number regime, the electric field induced by an electrode,[18] and in the present paper we describe a prototype, two-dimensional code in which we relax the assumption of quasi-neutrality to examine the plasma sheaths present on electrode surfaces. Accurate modeling of the voltage drop and dissipative heating present in the electrode sheaths will be required to evaluate the feasibility of proposed electromagnetic flow control schemes.

*Research Aerospace Engineer, Air Vehicles Directorate, AFRL/VAAC, 2210 Eighth Street. Senior Member AIAA.

†Senior Research Aerospace Engineer, Air Vehicles Directorate, AFRL/VAAC, 2210 Eighth Street. Associate Fellow AIAA.

Plasma Sheaths

Because the electric force due to even a small percentage imbalance of charged particles is so strong, any excess charge is quickly eliminated by particle motion, and quasi-neutrality is usually an excellent approximation in relatively high-density, low-temperature plasmas. Quasi-neutrality does not prevail, however, for ionized gas in the vicinity of a solid surface. This region is called a plasma sheath.[19,20]

A relatively cold wall tends to function as a sink for charged particles, because it catalyzes recombination reactions and retains or absorbs charged particles at its surface. In order to balance the flow of positive and negative charge carriers to the wall, an electric field, generated by charge separation, must inhibit the flow of the more mobile species.

In an electropositive plasma (one with few negative ions), negative charge is carried predominantly by electrons, which have a very much higher mobility than the positive ions. The solid boundary, in this case, must have a potential more negative than the bulk plasma, in order to repel the electrons. The characteristic length scale of the layer of charge separation is on the order of the electron Debye length: $\lambda_{De} = (\epsilon_0 k_B T_e / n_e e^2)^{1/2}$. This distance can range over several orders of magnitude in typical engineering applications. In a typical glow discharge,[20] the electron temperature lies in the range of 1-10 eV ($10^4 - 10^5$ K) and the electron number density varies from 10^{14} m^{-3} to 10^{19} m^{-3}, for total gas pressures in the range $10^{-3} - 1$ torr ($10^{-6} - 10^{-3}$ Pa). For 1 eV, the corresponding Debye length varies from 1 mm at the lowest number density to 1 μm in the high density range. This wide variation in length scale relative to the mean free path and to typical dimensions of an experimental system complicates numerical modeling of the sheath region.

Several levels of modeling have been used to approach the sheath problem, and plasmadynamics in general.[20–22] At a rather fundamental level, a plasma can be treated as a collection of particles; the resulting mathematical model is solved by Particle-in-Cell Monte Carlo Collision (PIC MCC) methods. The macroscopic properties of the plasma are determined from the statistical behavior of the particles. These models are very general, and are well suited to treating certain rarefied gas phenomena, such as stochastic heating. The computational cost of PIC MCC methods becomes very great, however, as the number of particles and collision rate increase.

At a higher level of modeling, the generalized Boltzmann equation is solved for the particle distribution function. This level of modeling can also be computationally expensive, since there are seven independent variables (particle position, particle velocity, and time). Solutions of the Boltzmann equation can, for example, be used to treat the high degree of thermodynamic nonequilibrium for the electrons in glow discharges.

At a third level of modeling, conservation equations for particle identity, momentum, and energy can be derived by taking moments of the Boltzmann equation. This can be done for each species to form a multi-fluid model, or for the gas as a whole to obtain a magnetohydrodynamic model. In the present paper, we will examine multi-fluid models at different levels of approximation. In future work, we plan to examine patching a sheath model to a single-fluid computation (*e.g.*, see Ref. 23).

Numerical Model

A prototype two-dimensional code was written to solve the continuum conservation equations of mass (or particle identity), momentum, and energy for an arbitrary number of species. These equations can be cast in the following generic form for an arbitrary species k:

$$\frac{\partial n_k}{\partial t} + \nabla \cdot (n_k \vec{u}_k) = \omega_k, \qquad (1)$$

$$\frac{\partial}{\partial t}(\rho_k \vec{u}_k) + \nabla \cdot (\rho_k \vec{u}_k \vec{u}_k - \mathbf{\Sigma}_k) = \vec{f}_k + \vec{K}_k, \qquad (2)$$

$$\frac{\partial \mathcal{E}_k}{\partial t} + \nabla \cdot (\vec{u}_k \mathcal{E}_k - \mathbf{\Sigma}_k \cdot \vec{u}_k + \vec{Q}_k) = P_k + H_k. \qquad (3)$$

Here n_k is the number density, $\rho_k = m_k n_k$ is the mass density, $\vec{u}_k$ is the mean velocity, and $\mathcal{E}_k = \rho_k(\epsilon_k + u_k^2/2)$ is the total energy. The terms $\vec{K}_k$ and H_k are sources representing momentum and energy exchange between species due to collisions; ω_k is the rate of creation of particles of species k due to chemical reactions. The total stress tensor is $\mathbf{\Sigma}_k$ and the heat flux vector is $\vec{Q}_k$. The force and power delivered to species k by the electromagnetic field are $\vec{f}_k = \zeta_k \vec{E} + \vec{j}_k \times \vec{B}$ and $P_k = \vec{j}_k \cdot \vec{E}$, where $\zeta_k = q_k n_k$ is the charge density, $\vec{j}_k = q_k n_k \vec{u}_k$ is the electric current, $\vec{E}$ is the electric field, and $\vec{B}$ is the magnetic field (which we take to be zero in the present work). An appropriate summation applied to Eqs. (1)-(3) leads to the usual single-fluid conservation equations.

In this paper, Eqs. (1)-(3) are solved in different forms, under various simplifications. All these forms are conservation equations that may be written in flux vector form as:

$$\frac{\partial U}{\partial t} + \frac{\partial E}{\partial x} + \frac{\partial F}{\partial y} = \frac{\partial E_v}{\partial x} + \frac{\partial F_v}{\partial y} + S, \qquad (4)$$

where the fluxes have been separated into convective and diffusive (subscript v) terms. The governing equations are extended to curvilinear coordinates in the standard manner[24] by introducing the transformation $x = x(\xi,\eta)$, $y = y(\xi,\eta)$. The strong conservation form is employed, transforming Eq. (4) to:

$$\frac{\partial U'}{\partial t} + \frac{\partial E'}{\partial \xi} + \frac{\partial F'}{\partial \eta} = \frac{\partial E'_v}{\partial \xi} + \frac{\partial F'_v}{\partial \eta} + S', \qquad (5)$$

where, with J representing the Jacobian of the transformation, $U' = U/J$, $S' = S/J$,

$$\begin{aligned} E' &= (\xi_x E + \xi_y F)/J, \\ F' &= (\eta_x E + \eta_y F)/J, \end{aligned}$$

and analogous forms for the diffusive terms. The metrics were computed with second order spatial accuracy.

The fluid equations were solved using MacCormack's explicit, second-order predictor-corrector method.[24] Fourth-order damping was applied to stabilize the solution when necessary.

Assuming that the magnetic field is zero, Maxwell's equations reduce to:

$$\nabla \times \vec{E} = 0, \tag{6}$$

$$\nabla \cdot \vec{E} = \zeta/\epsilon_0, \tag{7}$$

where $\zeta = \sum_k q_k n_k$ is the total charge density. Introducing a potential $\vec{E} = -\nabla\Phi$, we obtain Poisson's equation:

$$\nabla^2\Phi = -\zeta/\epsilon_0. \tag{8}$$

In two dimensions, we write Poisson's equation as:

$$\frac{\partial^2\Phi}{\partial x^2} + \frac{\partial^2\Phi}{\partial y^2} = R. \tag{9}$$

In transformed space, this becomes:

$$\frac{\partial G}{\partial \xi} + \frac{\partial H}{\partial \eta} = R', \tag{10}$$

where

$$\begin{aligned} G &= \left[(\xi_x^2 + \xi_y^2)\Phi_\xi + (\xi_x\eta_x + \xi_y\eta_y)\Phi_\eta\right]/J, \\ H &= \left[(\xi_x\eta_x + \xi_y\eta_y)\Phi_\xi + (\eta_x^2 + \eta_y^2)\Phi_\eta\right]/J, \end{aligned}$$

and $R' = R/J$. The equations were discretized using second order spatial differences. The Poisson equation was solved using an alternating direction implicit (ADI) method with successive over-relaxation (SOR).[24] The resulting tridiagonal matrices were solved using the Thomas algorithm.

In the problems considered in this paper, the electrons were assumed to be in Boltzmann equilibrium with the electric field: $n_e = n_0 \exp(e\Phi/k_B T_e)$, with a constant electron temperature T_e, and a reference number density n_0 corresponding to $\Phi = 0$. This assumption makes the right hand side of the Poisson equation nonlinear. Following Ref. 25, this term was linearized to improve computational efficiency:

$$R = R_{\text{old}} - \frac{e^2 n_e(\Phi_{\text{old}})}{\epsilon_0 k_B T_e}\left(\Phi - \Phi_{\text{old}}\right). \tag{11}$$

Here the subscript 'old' indicates evaluation with values known from the previous step in the SOR procedure.

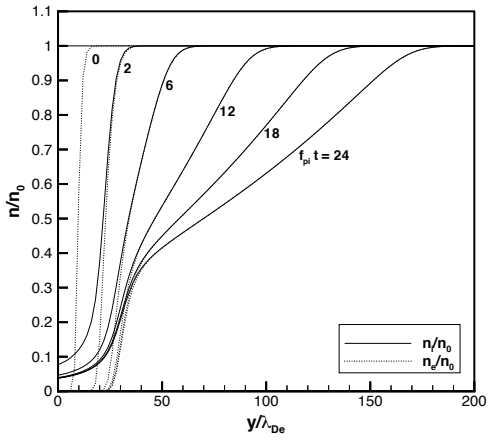

a) Number density.

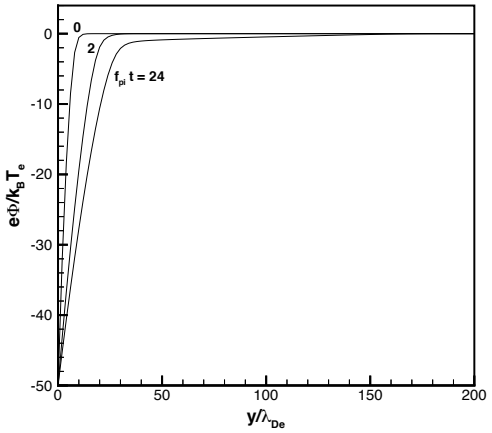

b) Electric potential.

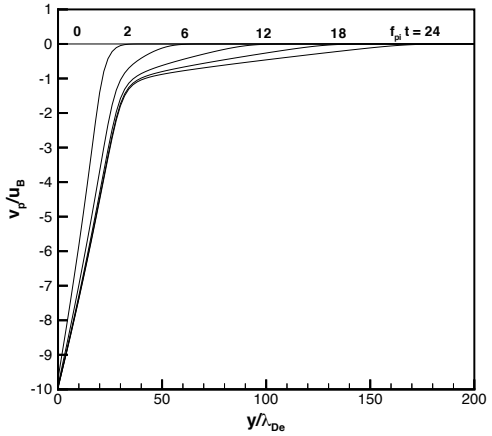

c) Ion velocity.

Fig. 1 Evolution of transient plasma sheath.

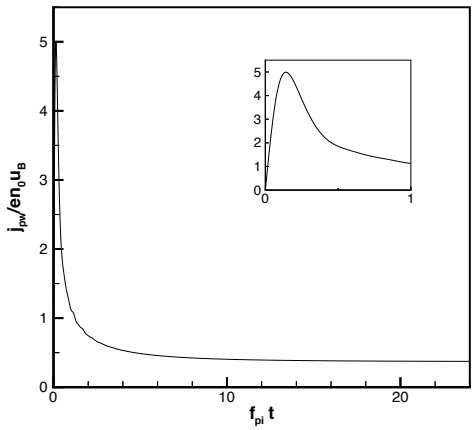

Fig. 2 Ion current at electrode.

Transient Plasma Sheath

As a test of the coupled fluid and potential equations, we examine the effect of a suddenly-applied electrode potential on a initially uniform, low-density plasma. The resulting transient plasma sheath was first observed in studies of ion-acoustic waves generated by impulsive electrode voltages,[26] and has received recent attention in the context of plasma-source ion implantation.[20]

Here we replicate the computations of Widner *et al.*,[27] who found good agreement between the cold ion model and a set of experiments carried out in xenon gas, with a background gas pressure of $p = 0.5$ mtorr (0.07 Pa). The electron temperature in the experiments was on the order of 1 eV ($T_e = 11600$ K), and the neutral gas temperature was near room temperature ($T_e/T_p \sim 20$). The charged particle density in the bulk plasma was in the range of $10^{14} - 10^{15}$ m^{-3}.

We consider a collisionless, cold ion model. The conservation of particle identity and momentum for the ions are expressed as:

$$\frac{\partial n_p}{\partial t} + \nabla \cdot (n_p \vec{u}_p) = 0, \tag{12}$$

$$\frac{\partial}{\partial t}(n_p \vec{u}_p) + \nabla \cdot (n_p \vec{u}_p \vec{u}_p) = e n_p \vec{E}/m_p. \tag{13}$$

The electrons are taken to be in Boltzmann equilibrium:

$$n_e = n_0 \exp(e\Phi/k_B T_e), \tag{14}$$

where the electron temperature T_e is taken to be constant. The electric field is given by $\vec{E} = -\nabla\Phi$, and the potential is found from:

$$\nabla^2 \Phi = -e(n_p - n_e)/\epsilon_0. \tag{15}$$

The conditions in the bulk plasma are $\vec{u}_p = 0$, $n_e = n_p = n_0$ and $\Phi = 0$.

In the present computations, the domain was taken to be $0.05\lambda_{De} \times 200\lambda_{De}$ in a uniform grid of 6×101 points, and the time step was $f_{pi}\Delta t = 0.01$, where $2\pi f_{pi} = (n_0 e^2/\epsilon_0 m_p)^{1/2}$ is the ion plasma frequency. The initial condition was taken to be uniform, and a potential of $e\Phi/k_B T_e = -50$ was suddenly applied at $t = 0$. The results of the computations are shown in Fig. 1. The data are normalized by the bulk plasma density n_0, the Debye length λ_{De}, and the Bohm velocity $u_B = (k_B T_e/m_p)^{1/2}$.

Figure 1a shows the distribution of ion and electron number densities in the sheath. The results are essentially identical to those obtained by Widner *et al.* with a different numerical scheme. With the sudden application of a large negative potential, the electrons are repelled from the electrode forming a layer of positive charge. The relatively massive ions slowly respond to the changed conditions, forming an ion current into the electrode. As a result, the space charge diminishes, and the sheath region expands into the bulk plasma, gradually approaching a steady-state. Ahead of the charge separation in the sheath is a quasi-neutral region, an unsteady presheath. The edge of the presheath propagates into the bulk plasma at the ion acoustic speed, in a manner somewhat analogous to an unsteady expansion wave in neutral gasdynamics.

The limited propagation of the sheath into the bulk plasma is seen again in Fig. 1b, which shows the time-evolution of the electric potential. After the initial transient sheath evolution, the potential shows strong variation in the sheath ($x/\lambda_{De} < 35$), and lesser variation in the presheath. Corresponding behavior is seen in the ion velocity distribution (Fig. 1c). The unsteady presheath is seen to accelerate the ions from the bulk plasma up to approximately the Bohm velocity, supporting a nearly steady sheath.

The current to the wall comes from the charges uncovered by the expanding rarefaction wave. The ion current at the electrode $en_p|v_p|$ is shown in Fig. 2. There is an initial surge in current (see the inset in the figure) as the transient sheath forms, followed by a gradual relaxation to a constant current density at large times.

Transient Sheath at High Density

In the rarefied regime considered in the previous section, ion motion was determined by a balance between inertia and the electric force. At the opposite extreme of density, ion inertia is negligible, and ion motion is determined by a balance of the electric force, the ion pressure gradient, and collisional drag with the neutral gas. The resulting model is a system of diffusion equations.

For simplicity, we again neglect chemical reactions, but this is a more severe restriction in the high-density regime. The particle conservation equation is:

$$\frac{\partial n_p}{\partial t} + \nabla \cdot \vec{\Gamma}_p = 0. \tag{16}$$

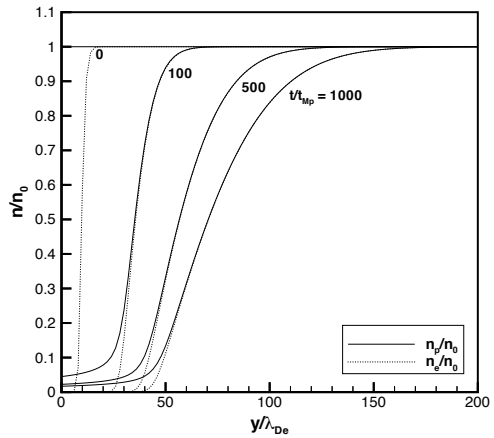

a) Number density.

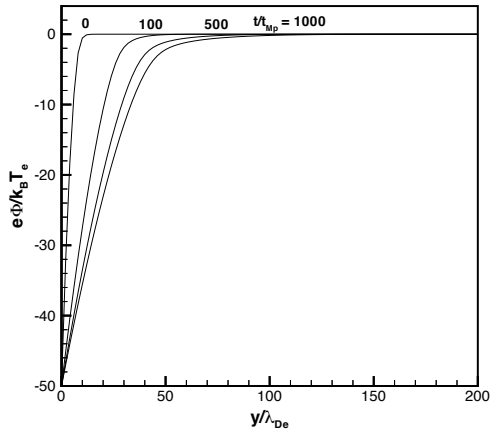

b) Electric potential.

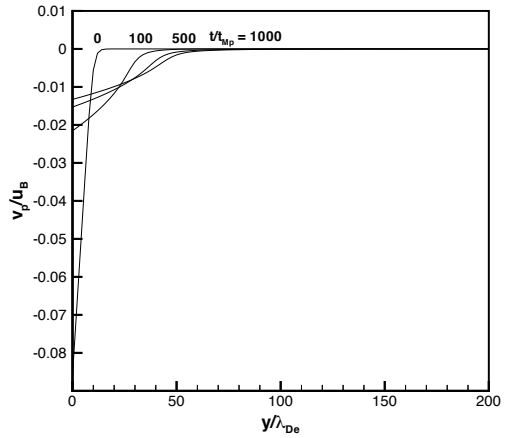

c) Ion velocity.

Fig. 3 Evolution of transient plasma sheath under diffusion model.

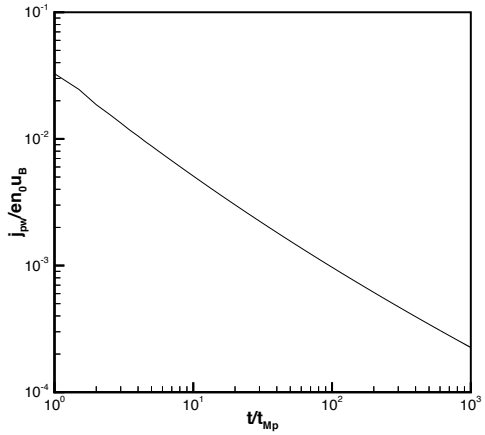

Fig. 4 Ion current at electrode under diffusion model.

The corresponding momentum equation is:

$$\vec{\Gamma}_p = n_p \mu_p \vec{E} - D_p \nabla n_p. \tag{17}$$

For simplicity, the ion temperature is taken to be uniform, and equal to the neutral gas temperature. The working fluid was taken to be argon. The neutral gas state was $p = 100$ torr (13.3 kPa) and $T = 0.1$ eV (1160 K) and the electron temperature was $T_e = 1$ eV (11600 K). The ion mobility was taken to have the constant value of $\mu_p = 10^{-3}$ m^2/V$\cdot$s, and the corresponding diffusion coefficient was $D_p = 10^{-4}$ m^2/s. The electron density and the Poisson equation have the same form as in the previous problem, Eqs. (14)-(15).

The computational domain was taken to be $0.05\lambda_{De} \times 200\lambda_{De}$ in a uniform grid of 3×101 points. The time step was $\Delta t/t_{Mp} = 0.5$, where $t_{Mp} = \epsilon_0/en_p\mu_p$ is the Maxwell time scale for the ions.[21] The initial condition was taken to be uniform, with the following conditions in the bulk plasma: $\vec{u}_p = 0$, $n_e = n_p = n_0$ and $\Phi = 0$. A potential of $e\Phi/k_BT_e = -50$ was suddenly applied at $t = 0$.

The evolution of the high-density sheath is illustrated in Fig. 3. The character of the solution reflects the change of the governing equations from the hyperbolic form examined in the previous section to a parabolic form here. In the low-density regime, a wave propagates away from the electrode at the ion-acoustic speed, carrying the first signal of the change in electrode conditions. In the present case, the signal of the applied cathode voltage is carried by an advancing diffusion front, a much slower process. Rather than approaching a steady-state, the charge separation is seen to decay continuously as the sheath expands. The characteristic ion velocity is now significantly smaller than the Bohm velocity (Fig. 3c). One feature in common with the rarefied gas case is the separation of the solution into a sheath with charge separation and a presheath with near charge-neutrality.

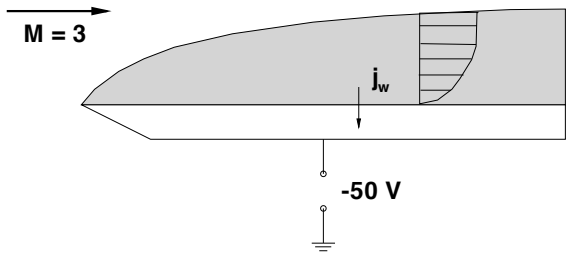

Fig. 5 Schematic diagram of boundary layer problem.

The ion current at the electrode is shown in Fig. 4. In contrast with the previous case, shown in Fig. 2, the current decays continuously with time, and has a significantly smaller magnitude.

Boundary Layer Flow

Plasma sheaths are expected to have a significant influence on the boundary layer flow over electrode surfaces in aerospace applications. Shneider *et al.*,[28] for example, found a significant cathode voltage drop and sheath thickness in a simplified analysis of the flow in a hypersonic MHD channel (1-D sheath calculation based on independently-computed fluid boundary layer solutions). Here we present a preliminary study of a fully-coupled solution for supersonic flow over a cathode.

We solve the full two-dimensional Navier-Stokes equations with force and energy source terms, along with advection-diffusion equations for the ions and a Poisson equation for the electric potential. To reduce computational effort in this preliminary work, we assume the electrons are in Boltzmann equilibrium with the electric potential, and do not treat chemical reactions or an imposed magnetic field.

A schematic diagram of the problem is shown in Fig. 5. A uniform, Mach 3 argon flow approaches a conductive plate from the left. The plate is assumed to be maintained at a constant potential of -50 V. The plate acts as a cathode, drawing a positive current density j_w, which is balanced by the freestream plasma entrained by the growing fluid boundary layer (grey shaded region). The no-slip condition is enforced at the plate, with either a cooled (constant temperature) wall or an adiabatic wall.

The conservation of mass, momentum, and energy for the overall gas are expressed as:

$$\frac{\partial \rho}{\partial t} + \nabla \cdot (\rho \vec{u}) = 0, \tag{18}$$

$$\frac{\partial}{\partial t}(\rho \vec{u}) + \nabla \cdot (\rho \vec{u}\vec{u} - \mathbf{\Sigma}) = \zeta \vec{E}, \tag{19}$$

$$\frac{\partial \mathcal{E}}{\partial t} + \nabla \cdot (\vec{u}\mathcal{E} - \mathbf{\Sigma} \cdot \vec{u} + \vec{Q}) = \vec{E} \cdot \vec{j}, \tag{20}$$

where $\mathcal{E} = \rho(\epsilon + u^2/2)$ is the total fluid energy per unit mass, the net charge is $\zeta = e(n_p - n_e)$, and the current density is $\vec{j} = \zeta \vec{u} + e\vec{\Gamma}_p$. The usual constitutive equations for the stress and heat flux in a Newtonian fluid were employed:

$$\Sigma_{ij} = -p\delta_{ij} + \mu_v \left(\frac{\partial u_i}{\partial x_j} + \frac{\partial u_j}{\partial x_i} \right) + \lambda_v \frac{\partial u_k}{\partial x_k} \delta_{ij}, \tag{21}$$

and

$$Q_i = -k_t \frac{\partial T}{\partial x_i}. \tag{22}$$

Values of the viscosity and thermal conductivity were taken from the correlations in White.[29] We assume an ideal gas with constant specific heats: $p = \rho RT$ and $\epsilon = C_v T$.

The equations for particle conservation and momentum conservation for the ions are:

$$\frac{\partial n_p}{\partial t} + \nabla \cdot (n_p \vec{u} + \vec{\Gamma}_p) = 0, \tag{23}$$

$$\vec{\Gamma}_p = n_p \mu_p \vec{E} - D_p \nabla n_p. \tag{24}$$

The ion mobility was taken from the correlation given in Boeuf and Pitchford,[30] and the diffusion coefficient was determined from the Einstein relation.

The electrons are taken to be in Boltzmann equilibrium:

$$n_e = n_\infty \exp(e\Phi / k_B T_e), \tag{25}$$

where the electron temperature T_e is constant, and the potential is referenced to the freestream. The electric field is given by $\vec{E} = -\nabla\Phi$, and the potential is found from:

$$\nabla^2 \Phi = -\zeta/\epsilon_0. \tag{26}$$

As a preliminary step, the code was validated for a neutral gas boundary layer flow. The results are shown in Fig. 6, for a grid of 31×61 points and a 0.3 m long plate. The freestream conditions were $M_\infty = 3$, $T_\infty = 200$ K, and $p_\infty = 21.5$ kPa (161 torr), corresponding to stagnation conditions of $T_0 = 800$ K and $p_0 = 689$ kPa. For the cold wall case, Fig. 6a, we see a typical laminar boundary layer velocity profile. A bulge in the temperature profile corresponds to the presence of significant viscous dissipation at this Mach number. For the insulated wall case shown in Fig. 6b, we see a temperature rise at the wall corresponding to the adiabatic wall temperature. The boundary layer thickness is significantly greater for this case, as a result of the significantly higher temperatures and lower densities in the boundary layer.

Figure 7 shows the results of calculations for an ionized flow. The freestream Mach number, temperature, and pressure are the same as in the previous example. The electron temperature was taken to be 1 eV ($T_e = 11600$ K), the electrode potential was $\Phi_w = -50$ V, and the wall temperature was taken to be equal to the freestream temperature. Figure 7a corresponds to a freestream plasma density of $n_\infty = 1.0 \times 10^{17}$ m^{-3}, whereas Fig. 7b corresponds to $n_\infty = 1.0 \times 10^{20}$ m^{-3}.

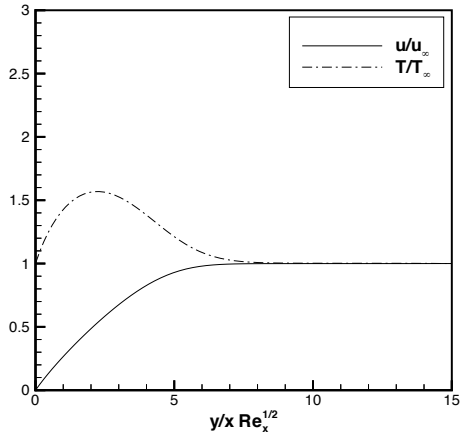

a) Cold wall, $T_w = T_\infty$.

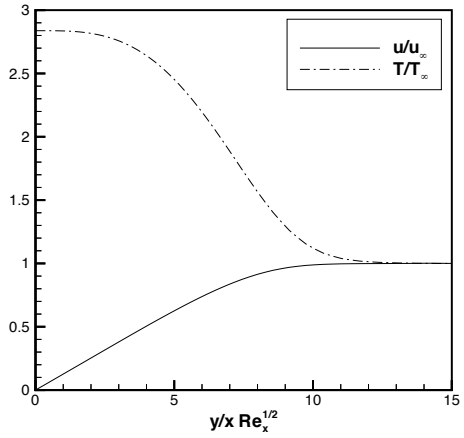

b) Adiabatic wall, $(\partial T/\partial y)_w = 0$.

Fig. 6 Profiles of temperature and the streamwise component of velocity in the boundary layer for the neutral gas case ($x = 0.3$ m).

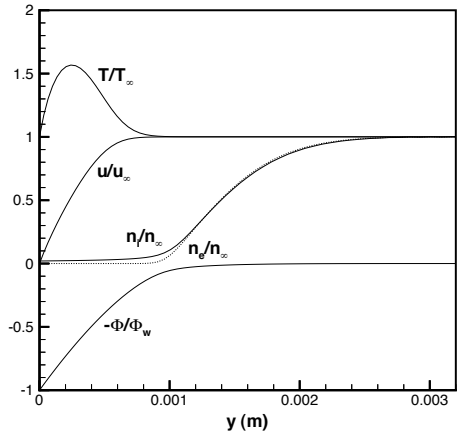

a) Thick sheath, $n_\infty = 1.0 \times 10^{17}$ m^{-3}.

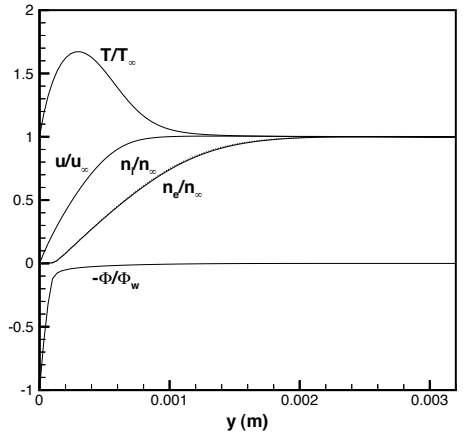

b) Thin sheath, $n_\infty = 1.0 \times 10^{20}$ m^{-3}.

Fig. 7 Cathode boundary layer profiles at $x = 0.3$ m.

Due to the dependence of the Debye length on the electron number density, the sheath is thicker in the former case.

Both solutions have much in common with the simple diffusion problem considered previously (Fig. 3). The sheath region near the electrode is characterized by charge separation and relatively weak number density gradients. There is a correspondingly large electric field $-\partial\Phi/\partial y$. Far from the electrode, the number density gradients are relatively large, but the charge separation is very small. A relatively weak electric field is present there. The two regions are seen to meet in a transition layer at the sheath edge. One difference from the previous diffusion problem is that a steady state is reached in the boundary layer flow, since the ion current drawn by the electrode is balanced by freestream plasma captured by the growing boundary layer.

For the case with relatively weaker ionization (Fig. 7a), the velocity and temperature profiles are indistinguishable from the corresponding neutral gas case (Fig. 6a). Somewhat higher temperatures, and a slightly modified velocity profile, are present in the case with stronger ionization (Fig. 7b). These differences are a result of dissipative heating from the larger ion current present with higher electron density.

Summary and Future Work

Preliminary results are presented from a study of plasma sheaths at the surface of electrodes immersed in hypersonic flow. A two-dimensional numerical code was written in which the conservation laws of fluid dynamics were solved with an explicit finite difference scheme and a Poisson equation for the electric potential was solved simultaneously using an SOR/ADI method. Three example problems were considered: a transient plasma sheath in the collisionless, cold-ion regime, an analogous sheath in the diffusion regime,

and a supersonic, laminar, boundary layer flow over a cathode. Good agreement was found between the collisionless sheath computation and a solution available in the literature. A significant voltage drop and temperature rise were observed in the electrode boundary layer flow; these effects are expected to be important in flow control applications. Future work will focus on implementing an implicit numerical scheme, and on enhancing the fidelity of the physical model.

Acknowledgments

This project was sponsored by the Air Force Office of Scientific Research, and monitored by Drs. W. Hilbun and J. Schmisseur. This work was also supported in part by a grant of High Performance Computing time from the Department of Defense Major Shared Resource Center at The Naval Oceanographic Office (NAVO). The authors would also like to acknowledge useful interaction with Profs. W. Bailey and M. Hughson of the Air Force Institute of Technology.

References

[1]Rossow, V. J., "On Flow of Electrically Conducting Fluids Over a Flat Plate in the Presence of a Transverse Magnetic Field," NACA Report 1358, National Advisory Committee for Aeronautics, Washington, DC, March 1957.

[2]Ziemer, R. W. and Bush, W. B., "Magnetic Field Effects on Bow Shock Stand-off Distance," *Physical Review Letters*, Vol. 1, No. 2, 1958, pp. 58–59.

[3]Wilkinson, J. B., "Magnetohydrodynamic Effects on Stagnation-Point Heat Transfer from Partially Ionized Nonequilibrium Gases in Supersonic Flow," *Engineering Aspects of Magnetohydrodynamics: Proceedings, 3rd Symposium*, edited by N. W. Mather and G. W. Sutton, Gordon and Breach Science Publishers, New York, 1964, pp. 413–438.

[4]Seeman, G. R. and Cambel, A. B., "Observations Concerning Magnetoaerodynamic Drag and Shock Standoff Distance," *Proceedings of the National Academy of Sciences*, Vol. 55, No. 3, 1966, pp. 457–465.

[5]Romig, M. F., "The Influence of Electric and Magnetic Fields on Heat Transfer to Electrically Conducting Fluids," *Advances in Heat Transfer*, edited by T. F. Irvine and J. P. Hartnett, Academic Press, New York, 1964, pp. 267–354.

[6]Klimov, A. I., Koblov, A. N., Mishin, G. I., Serov, Y. L., and Yavor, I. P., "Shock Wave Propagation in a Glow Discharge," *Soviet Technical Physics Letters*, Vol. 8, No. 4, 1982, pp. 192–194.

[7]Ganguly, B. N., Bletzinger, P., and Garscadden, A., "Shock Wave Damping and Dispersion in Nonequilibrium Low Pressure Argon Plasmas," *Physics Letters A*, Vol. 230, 1997, pp. 218–222.

[8]Gurijanov, E. P. and Harsha, P. T., "AJAX: New Directions in Hypersonic Technology," AIAA Paper 96-4609, November 1996.

[9]Voinovich, P. A., Ershov, A. P., Ponomareva, S. E., and Shibkov, V. M., "Propagation of Weak Shock Waves in Plasma of Longitudinal Flow Discharge in Air," *High Temperature*, Vol. 29, No. 3, 1991, pp. 468–476.

[10]Hilbun, W. M., *Shock Waves in Nonequilibrium Gases and Plasmas*, Ph.D. thesis, Air Force Institute of Technology, Wright-Patterson AFB, OH, October 1997.

[11]Poggie, J., "Energy Addition for Shockwave Control," AIAA Paper 99-3612, June 1999.

[12]Macheret, S. O., Ionikh, Y. Z., Chernysheva, N. V., Yalin, A. P., Martinelli, L., and Miles, R. B., "Shock Wave Propagation and Dispersion in Glow Discharge Plasmas," *Physics of Fluids*, Vol. 13, No. 9, 2001, pp. 2693–2703.

[13]Hoffmann, K. A., Damevin, H.-M., and Dietiker, J.-F., "Numerical Simulation of Hypersonic Magnetohydrodynamic Flows," AIAA Paper 2000-2259, June 2000.

[14]MacCormack, R. W., "A Conservation Form Method for Magneto-Fluid Dynamics," AIAA Paper 2001-0195, January 2001.

[15]Macheret, S. O., Shneider, M. N., and Miles, R. B., "External Supersonic Flow and Scramjet Inlet Control by MHD with Electron Beam Ionization," AIAA Paper 2001-0492, January 2001.

[16]Gaitonde, D. V., "Development of a Solver for 3-D Non-Ideal Magnetogasdynamics," AIAA Paper 99-3610, June 1999.

[17]Poggie, J. and Gaitonde, D. V., "Computational Studies of Magnetic Control in Hypersonic Flow," AIAA Paper 2001-0196, January 2001.

[18]Gaitonde, D. V. and Poggie, J., "Elements of a Numerical Procedure for 3-D MGD Flow Control Analysis," AIAA Paper 2002-0198, January 2002.

[19]Mitchner, M. and Kruger, C. H., *Partially Ionized Gases*, J. Wiley, New York, 1973.

[20]Lieberman, M. A. and Lichtenberg, A. J., *Principles of Plasma Discharges and Materials Processing*, J. Wiley, New York, 1994.

[21]Boeuf, J.-P. and Merad, A., "Fluid and Hybrid Models of Non Equilibrium Discharges," *Plasma Processing of Semiconductors*, edited by P. F. Williams, Kluwer, Dordrecht, the Netherlands, 1997, pp. 291–319.

[22]Choudhuri, A. R., *The Physics of Fluids and Plasmas: An Introduction for Astrophysicists*, Cambridge University Press, Cambridge, 1998.

[23]Nitschke, T. E. and Graves, D. B., "Matching an RF Sheath Model to a Bulk Plasma Model," *IEEE Transactions on Plasma Science*, Vol. 23, No. 4, 1995, pp. 717–727.

[24]Anderson, D. A., Tannehill, J. C., and Pletcher, R. H., *Computational Fluid Mechanics and Heat Transfer*, Hemisphere Publishing, New York, 1st ed., 1984.

[25]Emmert, G. A. and Henry, M. A., "Numerical Simulation of Plasma Sheath Expansion, with Applications to Plasma-Source Ion Implantation," *Journal of Applied Physics*, Vol. 71, No. 1, 1992, pp. 113–117.

[26]Alexeff, I., Jones, W. D., Lonngren, K., and Montgomery, D., "Transient Plasma Sheath - Discovered by Ion-Acoustic Waves," *The Physics of Fluids*, Vol. 12, No. 2, 1969, pp. 345–346.

[27]Widner, M., Alexeff, I., Jones, W. D., and Lonngren, K. E., "Ion Acoustic Wave Excitation and Ion Sheath Evolution," *The Physics of Fluids*, Vol. 13, No. 10, 1970, pp. 2532–2540.

[28]Shneider, M. N., Macheret, S. O., and Miles, R. B., "Electrode Sheaths and Boundary Layers in Hypersonic MHD Channels," AIAA Paper 99-3532, June 1999.

[29]White, F. M., *Viscous Fluid Flow*, McGraw-Hill, New York, 2nd ed., 1991.

[30]Boeuf, J. P. and Pitchford, L. C., "Two-Dimensional Model of a Capacitively Coupled RF Discharge and Comparisons with Experiments in the Gaseous Electronics Conference Reference Reactor," *Physical Review E*, Vol. 51, No. 2, 1995, pp. 1376–1390.